THE JOURNAL OF PHYSICAL CHEMISTRY B

Article

pubs.acs.org/JPCB

Surface Analysis of Ionic Liquids with and without Lithium Salt Using X-ray Photoelectron Spectroscopy

Tsutomu Kurisaki,*[,†] Daisaku Tanaka,[†] Yoshiki Inoue,[†] Hisanobu Wakita,[†,§] Babak Minofar,[‡,⊥] Shuhei Fukuda,[‡] Shin-ichi Ishiguro,[‡] and Yasuhiro Umebayashi[‡,⊥]

[†]Department of Chemistry, Faculty of Science, Fukuoka University, 8-19-1 Nanakuma, Jonan-ku, Fukuoka 814-0180, Japan

[‡]Department of Chemistry, Faculty of Science, Kyushu University, 6-10-1 Hakozaki, Higashi-ku, Fukuoka 812-8581, Japan

[§]Advanced Materials Institute, Fukuoka University, 8-19-1 Nanakuma, Jonan-ku, Fukuoka 814-0180, Japan

Supporting Information

ABSTRACT: X-ray photoelectron spectroscopy (XPS) was applied to a neat ionic liquid 1-ethyl-3-methylimidazolium bis(trifluoromethanesulfonyl)imide [EMI$^+$][Tf$_2$N$^-$] and its lithium salt solution at room temperature to clarify the composition and structure of its near-surface region. Core level peaks were recorded for Li 1s, N 1s, C 1s, F 1s, O 1s, S 2s, and S 2p. Valence band XPS spectra (0−40 eV binding energy) were also studied. The XPS spectra were analyzed using DV-Xα calculations. Results show that the planar type isomer of the EMI$^+$ cation is dominant at the near-surface region of EMI-Tf$_2$N. Results of XPS measurements show a spectrum of Li 1s in Li/EMI-Tf$_2$N. The proposed models for the preferred orientation of the ions exhibit good agreement with results obtained from the DV-Xα calculations.

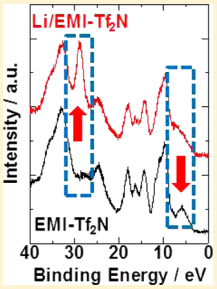

INTRODUCTION

Room-temperature ionic liquids have many attractive characteristics such as nonvolatility, extremely low vapor pressure, and nonflammability. These characteristics of ionic liquids enable their application to high-energy density electrochemical devices of high safety[1] such as lithium ion batteries,[2−4] fuel cells,[5−8] electric double-layer capacitors,[9−11] and dye-sensitized solar cells.[12−14] Numerous ionic liquid applications, particularly those using metal ions, have been described in the literature, and studies conducted from the perspective of fundamental science at a molecular level, examining the structure of ionic liquids and the coordination structure of metal ions in ionic liquids, are performed using various kinds of analysis methods such as ultraviolet photoelectron spectroscopy (USP),[15] metastable induced electron spectroscopy (MIES),[15] direct recoil spectroscopy (DRS),[16,17] and sum-frequency generation spectroscopy (SFG).[18−20]

X-ray absorption fine structure (XAFS) analysis can elucidate the local structure of the heavy metal ions in solution, although it is not so easy to apply that method to probe ions of light metal ions in solution. For solvation of a light metal ion, Raman spectroscopic analysis of lithium ion solvation has been reported in association with lithium ion batteries using ionic liquids composed of bis(trifluoromethanesulfonyl)amide (TFSA$^-$).[21−29] However, the lithium ion solvation number in ionic liquids has not been fully estimated from the observed spectra because the Raman spectra for the ionic liquids containing lithium ion, and even the neat ionic liquids themselves, are quite complicated. According to our previous studies, 1-ethyl-3-methylimidazolium (EMI$^+$) and TFSA$^-$ ion have conformational isomerism.[30−34] Moreover, two or three predominant conformers of the respective ions exist in equilibrium in the corresponding ionic liquid.

This report describes the lithium ion solvation structure and the component ion conformation in TFSA-based ionic liquids according to results obtained from Raman spectroscopy and DFT calculations[24,35] and a high-energy X-ray diffraction technique coupled with MD simulations.[36] These reports show that a lithium ion is coordinated by two TFSA$^-$ anions as a bidentate ligand. The anion in the first coordination sphere of the lithium ion prefers the cis conformation (two CF$_3$ groups locate at the cis position with respect to the S−N−S plane), although the trans one is a slightly favorable isomer in neat ionic liquid.

The liquid structure of ionic liquids influences several characteristics: the melting point, viscosity, ionic conductivity, etc. When ionic liquids are used for electrochemistry, it is extremely important that we understand the physicochemical properties and surface structures of ionic liquids[37−39] because their surfaces and interfaces play key roles in the multiphase reactions. In analyzing ionic liquid surfaces, it is necessary to analyze them under a clean surface. Therefore, ionic liquids must be analyzed under ultrahigh vacuum. Generally, X-ray photoelectron spectroscopy (XPS) is operated under ultrahigh vacuum. Therefore, the measured samples are solid state in almost all cases. XPS is a particularly powerful analytical tool that provides information related to both the elemental composition and the electronic structure of the element in solid samples. Such information would be extremely useful for

Received: February 20, 2012
Revised: July 31, 2012
Published: August 1, 2012

dx.doi.org/10.1021/jp301658k | J. Phys. Chem. B 2012, 116, 10870−10875

samples in solution, but the sample simply evaporates under the ultrahigh-vacuum conditions. Fortunately, ionic liquids show very low vapor pressure. Therefore, they can be measured *in situ* using XPS.[15,39−49] These studies have shown that the ionic liquids are stable during X-ray exposure and under ultrahigh-vacuum conditions. Furthermore, other prospects of XPS were found to be useful. XPS can reveal the composition of the surface layer, and it can also be used for purity analysis.[40−44] Moreover, angle-resolved XPS shows the surface orientation of the cation in the ionic liquids[48] and presents evidence that the dissolved complex is enriched in the ionic liquids.[49]

Surface structures of ionic liquids were studied using various side chains and anions with an imidazolium-based ionic liquid. Kimura et al. reported that the cis-confomer of bis-(trifluoromethanesulfonyl)imide (Tf_2N^-) anion is dominant among two stable conformers and that the anions are oriented with their CF_3 groups pointing toward the vacuum in the outermost molecular layer.[38] However, no report in the relevant literature describes the ionic liquid surface structure using an ionic liquid with dissolved metal ions.

This study investigated the electronic state of the lithium ion in ionic liquids to evaluate the liquid structure and solvation geometry around the lithium ion at the ionic liquid surface by the combination of XPS and discrete variational (DV)-Xα molecular orbital (MO) calculation method.

EXPERIMENTAL SECTION

Ionic Liquid Samples. The sample ionic liquid 1-ethyl-3-methylimidazolium bis(trifluoromethanesulfonyl)imide (EMI-Tf_2N) was prepared according to the literature.[41] An ionic liquid with $LiTf_2N$ salts dissolved by 0.5 mol kg^{-1} in EMI-Tf_2N was also prepared. The EMI^+ cation and Tf_2N^- anion structures of EMI-Tf_2N are presented in Figure 1. The water content was

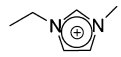

EMI^+:1-ethyl-3methyl imidazolium

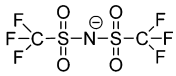

$Tf2N^-$:bis-(trifluoromethanesulfonyl)imide

Figure 1. Structures of ionic liquids investigated in this work.

checked using Karl Fischer titration to be less than 20 ppm after drying in a vacuum. All samples used for this study were stored in a high-performance glovebox (Miwa Mfg. Co. Ltd.), in which the water and oxygen contents were maintained below 1 ppm.

XPS. Ionic liquids were prepared by dropping them into a hole (3 mm diameter; 3 mm height) opened on an XPS liquid sample holder, made of molybdenum, after careful outgassing in a load lock system. Then they were introduced into the XPS chamber. The XPS measurements were conducted using a spectrometer (1800; PHI) with monochromatized Al Kα radiation. The X-ray source was operated at 14 kV and 400 W. The base pressure of the analytical chamber was typically ca. 1×10^{-7} Pa during XPS measurements. High-resolution spectra for N 1s and C 1s were curve fitted using software (XPSPEAK Ver. 4.1; Kwok, The Chinese University of Hong Kong). Curve fitting was performed using Gaussian shapes with Shirley-type background correction.[50] Ionic liquids appear to be very stable during exposure to the X-ray source because we have observed no evidence of vacuum down and beam damage to the sample. Our XPS measurement is conducted using a bulk ionic liquid. Therefore, the information on the near-surface region is provided from XPS measurements (see Results and Discussion, XPS survey spectra).

Calculations. The conformational isomers for EMI^+[30] cation and Tf_2N^- anion[31−33,35] have already been reported. For the EMI^+ cation, two isomers exist: one is planar type whose ethyl group combined with an imidazolium ring locates on the same plane of the imidazolium ring. The other is a nonplanar one whose ethyl group is in a nearly perpendicular direction to that of the ring. However, in the case of Tf_2N^- anion, two isomers of C1 and C2 type are also known. The calculation model for EMI^+ cation of nonplanar type was constructed from single-crystal structural data,[51] and that of the planar one was optimized using the Amsterdam Density Functional (ADF) program package.[52−54]

The calculation models for Tf_2N^- of C1 and C2 type were optimized using density functional theory (Gaussian 03 program package). In a previous study, we calculated theoretical spectra by a molecular orbital calculation using an isolated ion models.[55−57] These results show good agreement between observed XAFS spectra and calculated spectra. Figures 2 and 3 show those calculation models to be used DV-Xα

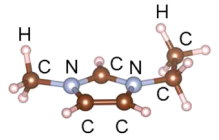

EMI^+: Planar type

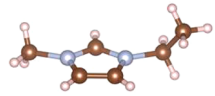

EMI^+: Non-planar type

Figure 2. Computational models of EMI^+ cations to be used for the DV-Xα calculation.

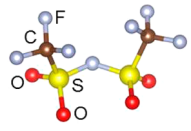

Tf_2N^-: C1 type

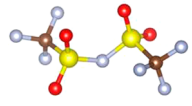

Tf_2N^-: C2 type

Figure 3. Computational models of Tf_2N^- anions to be used for the DV-Xα calculation.

molecular orbital calculation. For the DV-Xα calculation, numerical atomic orbitals of 1s, 2s, 2p, 3s, and 3p for nitrogen, and of 1s, 2s, and 2p for carbon, oxygen, and fluorine and of 1s, 2s, 2p, 3s, 3p, and 3d for sulfur, and orbital of 1s for hydrogen were used as a basis set for the calculations. For simulating the XPS spectra of EMI^+ and Tf_2N^-, we evaluated the respective densities of states (DOSs) by the DV-Xα calculation for

dx.doi.org/10.1021/jp301658k | J. Phys. Chem. B 2012, 116, 10870−10875

corresponding models. The calculated DOS is obtained by broadening the calculated MOs with 0.5 eV fwhm.

RESULTS AND DISCUSSION

XPS Survey Spectra. We measured XPS spectra (0−1000 eV) to examine the constituent elements in the ionic liquids (EMI-Tf_2N and Li/EMI-Tf_2N). The survey spectra are presented in the Supporting Information (Figure SI-1). Because a peak derived from the sample holder (Mo) did not appear to the XPS survey spectra, we estimate a sample thickness over 10 nm.[48] However, the general XPS measurement can give the information within approximately several nanometers from the surface. Therefore, our measurement obtains the information about the near-surface region of several nanometers from the surface. The observed XPS spectrum of EMI-Tf_2N agrees with that of Li/EMI-Tf_2N except for peak of Li 1s. For all spectra presented in this report, the *Y*-axis shows the intensity, in arbitrary units, and the *X*-axis shows the binding energy. From these XPS survey spectra, two peaks of silicon which were not included in the composition of ionic liquids were confirmed at 100 eV (Si 2p), and 150 eV (Si 2s) in both samples. This result demonstrates that the measured samples were contaminated with silicon grease during synthesis of the ionic liquid samples. Detailed analyses of the Si contamination in ionic liquids have been described elsewhere by Gottfried et al.[43]

XPS High-Resolution Spectra. *Core Level Peak.* We observed the XPS spectra of Li 1s, N 1s, C 1s, F 1s, O 1s, S 2s, and S 2p for both samples. C 1s XPS spectra were compared with the calculated C 1s spectra using the DV-Xα calculation. Because the observed XPS spectra of F 1s, O 1s, S 2s, and S 2p showed no important difference of the peak position and peak shape, useful geometric information related to the isomers of cation and anion in ionic liquids was not obtained.

Lithium 1s. The Li 1s spectra of Li/EMI-Tf_2N and EMI-Tf_2N are portrayed in Figure 4. The theoretical abundance ratio

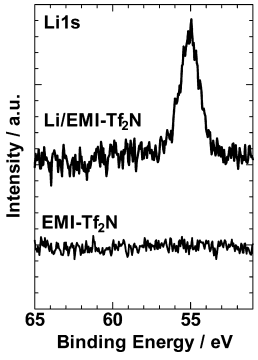

Figure 4. Observed XPS Li 1s spectra of Li/EMI-Tf_2N and EMI-Tf_2N.

of lithium in Li/EMI-Tf_2N (0.5 mol kg^{-1}) is about 0.3%. As a result, we can estimate that the Li 1s peak does not appear in the spectrum by the low concentration of 0.5 mol kg^{-1}. However, the Li 1s XPS spectrum of Li/EMI-Tf_2N sample exhibits a peak at 55 eV. This result suggests that lithium ion in EMI-Tf_2N sample is concentrated at the near-surface region of ionic liquids. Detailed discussion related to lithium ion concentrated by the near-surface region is described in the section presenting discussion of the valence band XPS spectra.

Nitrogen 1s. Two peaks appeared at 402 and 399 eV in observed N 1s XPS spectra of both samples (Figure 5). These peaks can be assigned to the respective nitrogen of EMI^+ cation

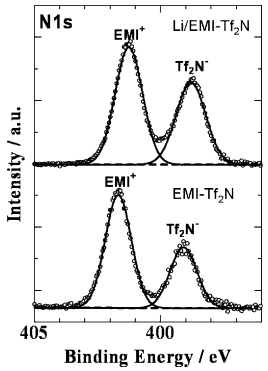

Figure 5. Observed XPS N 1s spectra of Li/EMI-Tf_2N and EMI-Tf_2N, including curve fitting results. These spectra consist of curve fitting (solid line), background (dashed line), and raw data (open circle) for each sample.

(402 eV) and Tf_2N^- anion (399 eV), as reported.[15,42] When we estimate the abundance ratio of the cation and the anion in both samples using the peak area ratio of both peaks, after having considered the existence ratio of the nitrogen atom of the cation and the anion in each sample, it is EMI^+:Tf_2N^- = 1.0:1.5 in the case of Li/EMI-Tf_2N, and EMI^+:Tf_2N^- = 1.0:1.1 in the case of EMI-Tf_2N. The result that the Tf_2N^- anion in an ionic liquid is concentrated by the near-surface region is similar to that reported by Kimura et al.[38] Therefore, we inferred that Tf_2N^- anion is concentrated in the near-surface region of Li/EMI-Tf_2N because the theoretical abundance ratio is EMI^+:Tf_2N^- = 1.0:1.2 in the case that $LiTf_2N$ salts is added to EMI-Tf_2N (0.5 mol kg^{-1}). Those results of Li 1s and N 1s XPS spectra indicated that $LiTf_2N$ salts are concentrated at the near-surface region in Li/EMI-Tf_2N.

Carbon 1s. The observed C 1s XPS spectra of EMI-Tf_2N and Li/EMI-Tf_2N are depicted in Figure 6. These spectra show

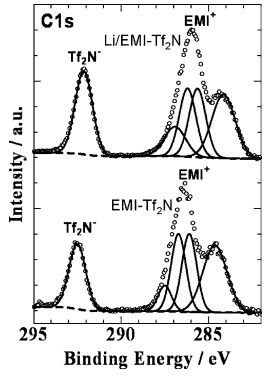

Figure 6. Observed XPS C 1s spectra of Li/EMI-Tf_2N and EMI-Tf_2N, including curve fitting results. These spectra consist of curve fitting (solid line), background (dashed line), and raw data (open circle) for each sample.

few differences of peak intensity and peak profile in C 1s spectra between both samples. Here, the binding energy values for the peak positions were determined by the fitted curves. We analyzed C 1s XPS spectra using data from the literature.[15,42] There are apparently four kinds of electronic states of carbons for EMI^+ cation and one kind of electronic state of carbon for Tf_2N^- anion in both of EMI-Tf_2N and Li/EMI-Tf_2N. In EMI-Tf_2N, two peaks at 287.5 and 286.7 eV were assigned to a signal of the carbon which was bonded to the two nitrogens in the

dx.doi.org/10.1021/jp301658k | J. Phys. Chem. B 2012, 116, 10870−10875

five-membered ring and a signal of carbon which was bonded to the one nitrogen in the ring, respectively. However, a peak at 286.1 eV is attributable to the two carbons of the methyl group and the ethyl group which were bonded directly to the nitrogen. Moreover, a peak at 284.7 eV is attributable to the carbon of the end ethyl group. They are the same results for Li/EMI-Tf_2N. Furthermore, the intensity of a peak at 284.7 eV, which was assigned to the carbon of the end ethyl group, increased about 2 times more than the predicted intensity for both samples. This result implies that the peak at 284.7 eV contains a peak of hydrocarbon group for silicone grease (Si contamination was described in the XPS survey spectra result). Figure 7 shows the C 1s calculated spectra from simulating the

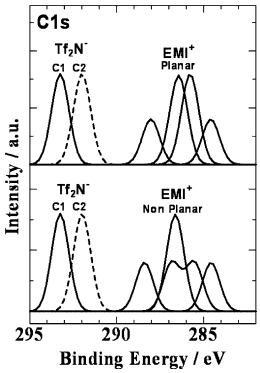

Figure 7. Calculated C 1s spectra of Li/EMI-Tf_2N and EMI-Tf_2N by the DV-Xα calculation. The top panel shows calculated spectra of the planar type model for EMI^+ cation (solid line) and the isomer model (C1 (solid line) and C2 (dashed line)). The bottom panel shows calculated spectra of nonplanar type model for EMI^+ cation (solid line) and the isomer model (C1 (solid line) and C2 (dashed line)).

XPS spectra. From analyzing the C 1s XPS spectra, we found that the planar type isomer reproduces the observed XPS spectra better than the nonplanar type isomer for EMI^+ cation, which suggests that the planar type isomer was contained more than nonplanar type isomer at the near-surface region in both samples. However, we were unable to identify the isomeric structure of Tf_2N^- anion for either sample.

Valence Band XPS Spectra (0–40 eV). The valence band XPS spectra (0–40 eV) were measured for the ionic liquids with and without $LiTf_2N$ (Figures 8 (1) and 8(1′)). When $LiTf_2N$ salts were added to EMI-Tf_2N, the peak at 28.9 eV increased and the peak at 5.9 eV decreased in XPS spectra of Li/EMI-Tf_2N. Those spectra show little difference of the peak profile in comparison with the valence band XPS spectra of lithium bis(trifluoromethanesulfonyl)imide $LiN(SO_2CF_3)_2$ salts.[58] Therefore, we believe that these spectra of the valence band are attributable to atomic orbitals of Tf_2N^- anion. We calculated the density of states (DOSs) spectra of only Tf_2N^- anion for the valence band (Figure 8). We described DOSs spectra for the valence band using the value of the photoionization cross section by Scofield[59] and curve fitting with the Gaussian function. We used two isomer models of C1 type (Figure 8(2)) and C2 type (Figure 8(2′)) for calculation. The total DOSs (heavy line) and the partial DOSs (thin line) are shown in the Supporting Information (Figure SI-2). Furthermore, Figure 8 presents a comparison of observed valence band XPS spectra of Li/EMI-Tf_2N (1) and EMI-Tf_2N (1′) and the calculated spectra of isomer models: C1 type (2) and C2 type (2′), for Tf_2N^- anion in the same region. We

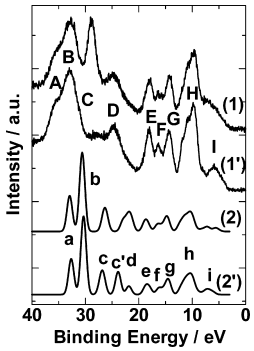

Figure 8. Comparison of observed XPS spectra of Li/EMI-Tf_2N (1) and EMI-Tf_2N (1′) in valence band region and calculated spectra of isomer models: C1 type (2) and C2 type (2′), for Tf_2N^- anion in valence band region by DV-Xα calculation. Each peak is marked by a sign (A–I and a–i). These spectra show the density of state (DOS) of total molecular orbitals (thin line) and the observed XPS spectra (heavy line).

were unable to obtain sufficient agreement of the peak position between the observed XPS spectra and the calculated DOS spectra in the valence band. Therefore, we cannot ascertain whether the structure of Tf_2N^- anion in ionic liquids is C1 type or C2 type. However, the peak profiles of calculated DOS spectra almost accord with these of observed XPS spectra, which suggests that the calculated DOS spectra are available for the peak constitution analysis of the observed XPS spectra. Therefore, the assignments of two peaks where the changes of intensity are shown in the observed XPS spectra (Figures 8(1) and 8(1′)) was performed using the calculated DOS spectra of C1 and C2 type (Figures 8(2) and 8(2′)). The peak positions and the assignment of observed XPS spectra of Li/EMI-Tf_2N and EMI-Tf_2N are shown in Table 1. In the peaks C and I in the observed XPS spectra, it is assigned to the peaks c, c′, and i in the calculated DOS spectra, respectively. Results show that the atomic orbitals of each peak consist of the following orbitals: peak c mainly consists of the O (54.0%) and S (42.2%), peak c′ of O (95.0%), and peak i of O (70.6%). This result indicates that the lithium ion in the ionic liquid was coordinated by the oxygen atoms in Tf_2N^- anion. Furthermore, the difference in the observed XPS spectra is not apparent except for peaks C and I. This is probably true because these peaks are constituted mainly by the atomic orbital, except for the oxygen atom.

The lithium ions in EMI-Tf_2N are believed to be coordinated to oxygen atoms in the Tf_2N^- anion. However, in EMI-Tf_2N, the EMI^+ cations are thought to interact via their C–H group with the oxygen in particular. The cation–anion interaction in Li/EMI-Tf_2N is changed as compared to EMI-Tf_2N. Therefore, the difference of the peak profile was shown in the observed XPS spectra. The Tf_2N^- anions in the near-surface region of ionic liquid increased as a result that solvated metal ions were localized on the near-surface region of EMI-Tf_2N. One report in the literature describes an investigation of the near-surface structure of the ionic liquid alkylimidazolium bis(trifluoromethanesulfonyl)amide.[60] When an alkyl chain is short, the Tf_2N^- anion is located in the near-surface region of the ionic liquids. Consequently, the lithium ions are located on the surface of the ionic liquid as a [Li-Tf_2N] because the lithium ions were coordinate to an anion.

dx.doi.org/10.1021/jp301658k | J. Phys. Chem. B 2012, 116, 10870–10875

Table 1. Peak Position and Assignment of Observed XPS Spectra of Li/EMI-Tf_2N and EMI-Tf_2N As Shown in Figure 8

peak positions of observed XPS spectra (eV)			atomic orbital and its proportion (%)					
peak	Li/EMI-Tf_2N	EMI-Tf_2N	peak	F	O	N	C	S
A	35.6	35.7	a	94.9	0.06	0.00	4.69	0.35
B	33.0	33.1	b	99.9	0.00	0.00	0.10	0.00
C	28.9		c	1.21	54.0	2.43	0.16	42.2
			c′	0.16	95.0	0.14	0.01	4.69
D	24.8	24.7	d	0.70	34.3	50.9	0.20	13.9
E	18.2	18.2	e	41.4	18.8	2.60	16.6	20.6
F	16.3	16.4	f	52.4	14.5	1.48	6.32	25.3
G	14.3	14.4	g	85.7	3.85	0.81	1.32	8.32
H	9.90	9.90	h	61.4	27.0	1.46	0.04	10.1
I	5.93	5.95	i	11.9	70.6	6.25	7.44	3.81

CONCLUSION

EMI-Tf_2N and Li/EMI-Tf_2N were studied using XPS at room temperature. Results show that the solvated lithium ions are confined to the near-surface region. Moreover, as judged from the N 1s core spectra, the Tf_2N^- anion concentration is higher than that of the EMI^+ cations; i.e., as a consequence of the lithium ion solvation, the cations are pushed away from the near-surface region. Taking these findings together, we report that the $LiTf_2N$ species are found mostly in the near-surface region. The C 1s spectra indicate that the planar EMI isomers dominate both in the neat ionic liquid and for lithium ion solvation. As concluded from the valence band XPS spectra (0−40 eV binding energy) and their analysis with DV-Xα calculation, the solvated lithium ions are coordinated to oxygen species of the Tf_2N^- anions. Results show that the C1 isomer of the Tf_2N^- anion is dominant at the near-surface region of EMI-Tf_2N. The Tf_2N^- anion is solvated as lithium ion with C1 isomer more easily than C2 isomer is. These results suggest that the lithium ion is concentrated in the near-surface region.

ASSOCIATED CONTENT

Supporting Information

Observed survey spectra of Li/EMI-Tf_2N and EMI-Tf_2N and the calculated DOSs spectra of Tf_2N^- anion for valence band region (Figures SI1 and SI2). This material is available free of charge via the Internet at http://pubs.acs.org.

AUTHOR INFORMATION

Corresponding Author

*Tel +81-92-871-6631; Fax +81-92-865-6030; e-mail kurisaki@fukuoka-u.ac.jp.

Present Address

[⊥]Graduate School of Science and Technology Niigata University, 8050, Ikarashi, 2-no-cho, Nishi-ku, Niigata City, 950-2181, Japan.

Notes

The authors declare no competing financial interest.

ACKNOWLEDGMENTS

This study was partially supported by Grants-in-Aid for Scientific Research Nos. P10750, 20350037, 22550088, 2200750, 23300319, 23350033, and 24655142 from the Japan Society for the Promotion of Science, and for Scientific Research in Priority Area (Ionic Liquids) No. 20031024 from MEXT Japan and Advanced Low Carbon Technology Research, and Development Program (ALCA) from Japan Science and Technology Agency (JST).

REFERENCES

(1) Ohno, H. *Electrochemical Aspects of Ionic Liquids*; John & Wiley Sons, Inc.: Hoboken, NJ, 2005.

(2) Sakaebe, H.; Matsumoto, H. *Electrochem. Commun.* **2003**, *5*, 594−598.

(3) Nakagawa, H.; Izuchi, S.; Kuwana, K.; Nukuda, T.; Aihara, Y. *J. Electrochem. Soc.* **2003**, *150*, A695−A700.

(4) Seki, S.; Kobayashi, Y.; Miyashiro, H.; Ohno, Y.; Usami, A.; Mita, Y.; Kihira, N.; Watanabe, M.; Terada, N. *J. Phys. Chem. B* **2006**, *110*, 10228−10230.

(5) Yoshizawa, M.; Xu, W.; Angell, C. A. *J. Am. Chem. Soc.* **2003**, *125*, 15411−15419.

(6) Xu, W.; Angell, C. A. *Science* **2003**, *302*, 422−425.

(7) Noda, A.; Susan, M. A. B. H.; Kudo, K.; Mitsushima, S.; Hayamizu, K.; Watanabe, M. *J. Phys. Chem. B* **2003**, *107*, 4024−4033.

(8) Susan, M. A. B. H.; Noda, A.; Mitsushima, S.; Watanabe, M. *Chem. Commun.* **2003**, 938−939.

(9) McEwen, A. B.; Ngo, H. L.; LeCompte, K.; Goldman, J. L. *J. Electrochem. Soc.* **1999**, *146*, 1687−1695.

(10) Ue, M.; Takeda, M. *J. Korean Electrochem. Soc.* **2002**, *5*, 192−196.

(11) Ue, M.; Takeda, M.; Toriumi, A.; Kominato, A.; Hagiwara, R.; Ito, Y. *J. Electrochem. Soc.* **2003**, *150*, A499−A502.

(12) Wang, P.; Zakeeruddin, S. M.; Comte, P.; Exnar, I.; Grätzel, M. *J. Am. Chem. Soc.* **2003**, *125*, 1166−1167.

(13) Wang, P.; Zakeeruddin, S. M.; Moser, J. E.; Nazeeruddin, M. K.; Sekiguchi, T.; Grätzel, M. *Nat. Mater.* **2003**, *2*, 402−407.

(14) Yamanaka, N.; Kawano, R.; Kubo, W.; Masaki, N.; Kitamura, T.; Wada, Y.; Watanabe, M.; Yanagida, S. *J. Phys. Chem. B* **2007**, *111*, 4763−4769.

(15) Höfft, O.; Bahr, S.; Himmerlich, M.; Krischok, S.; Schaefer, J. A.; Kempter, V. *Langmuir* **2006**, *22*, 7120−7123.

(16) Gannon, T. J.; Law, G.; Watson, P. R. *Langmuir* **1999**, *15*, 8429−8434.

(17) Law, G.; Watson, P. R.; Carmichael, A. J.; Seddon, K. R. *Phys. Chem. Chem. Phys.* **2001**, *3*, 2879−12885.

(18) Baldelli, S. *J. Phys. Chem. B* **2003**, *107*, 6148−6152.

(19) Iimori, T.; Iwahashi, T.; Ishii, H.; Seki, K.; Ouchi, Y.; Ozawa, R.; Hamaguchi, H.; Kim, D. *Chem. Phys. Lett.* **2004**, *389*, 321−326.

(20) Rivera-Rubero, S.; Baldelli, S. *J. Phys. Chem. B* **2006**, *110*, 15499−15505.

(21) Castriota, M.; Caruso, T.; Agostino, R. G.; Cazzanelli, E.; Henderson, W. A.; Passerini, S. *J. Phys. Chem. A* **2005**, *109*, 92−96.

(22) Lassègues, J.-C.; Grondin, J.; Talaga, D. *Phys. Chem. Chem. Phys.* **2006**, *8*, 5629−5632.

(23) Hardwick, L. J.; Holzapfel, M.; Wokaun, A.; Novák, P. *J. Raman Spectrosc.* **2007**, *38*, 110−112.

(24) Umebayashi, Y.; Mitsugi, T.; Fukuda, S.; Fujimori, T.; Fujii, K.; Kanzaki, R.; Takeuchi, M.; Ishiguro, S. *J. Phys. Chem. B* **2007**, *111*, 13028−13032.

(25) Duluard, S.; Grondin, J.; Bruneel, J.-L.; Pianet, I.; Grélard, A.; Campet, G.; Delville, M.-H.; Lassègues, J.-C. *J. Raman Spectrosc.* **2008**, *39*, 627−632.
(26) Lassègues, J.-C.; Grondin, J.; Aupetit, C.; Johansson, P. *J. Phys. Chem. A* **2009**, *113*, 305−314.
(27) Herstedt, M.; Henderson, W. A.; Smirnov, M.; Ducasse, L.; Servant, L.; Talaga, D.; Lassègues, J.-C. *J. Mol. Struct.* **2006**, *783*, 145−156.
(28) Herstedt, M.; Smirnov, M.; Johansson, P.; Chami, M.; Grondin, J.; Servant, L.; Lassègues, J.-C. *J. Raman Spectrosc.* **2005**, *36*, 762−770.
(29) Yamaguchi, T.; Mikawa, K.; Koda, S.; Fukazawa, H.; Shirota, H. *Chem. Phys. Lett.* **2012**, *521*, 69−73.
(30) Umebayashi, Y.; Hamano, H.; Tsuzuki, S.; Lopes, J. N. C.; Pádua, A. A. H.; Kameda, Y.; Kohara, S.; Yamaguchi, T.; Fujii, K.; Ishiguro, S. *J. Phys. Chem. B* **2010**, *114*, 11715−11724.
(31) Umebayashi, Y.; Mitsugi, T.; Fujii, K.; Seki, S.; Chiba, K.; Yamamoto, H.; Lopes, H. J. N. C.; Pádua, A. A. H.; Takeuchi, M.; Kanzaki, R.; Ishiguro, S. *J. Phys. Chem. B* **2009**, *113*, 4338−4346.
(32) Fujimori, T.; Fujii, K.; Kanzaki, R.; Chiba, K.; Yamamoto, H.; Umebayashi, Y.; Ishiguro, S. *J. Mol. Liq.* **2007**, *131*−*132*, 216−224.
(33) Umebayashi, Y.; Fujimori, T.; Sukizaki, T.; Asada, M.; Fujii, K.; Kanzaki, R.; Ishiguro, S. *J. Phys. Chem. A* **2005**, *109*, 8976−8982.
(34) Fujii, K.; Fujimori, T.; Takamuku, T.; Kanzaki, R.; Umebayashi, Y.; Ishiguro, S. *J. Phys. Chem. B* **2006**, *110*, 8179−8183.
(35) Umebayashi, Y.; Mori, S.; Fujii, K.; Tsuzuki, S.; Seki, S.; Hayamizu, K.; Ishiguro, S. *J. Phys. Chem. B* **2010**, *114*, 6513−6521.
(36) Umebayashi, Y.; Hamano, H.; Seki, S.; Minofar, B.; Fujii, K.; Hayamizu, K.; Tsuzuki, S.; Kameda, Y.; Kohara, S.; Watanabe, M. *J. Phys. Chem. B* **2011**, *115*, 12179−12191.
(37) Nakajima, K.; Ohno, A.; Hashimoto, H.; Suzuki, M.; Kimura, K. *J. Chem. Phys.* **2010**, *133*, 044702/1−044702/7.
(38) Nakajima, K.; Ohno, A.; Suzuki, M.; Kimura, K. *Langmuir* **2008**, *24*, 4482−4484.
(39) Hashimoto, H.; Ohno, A.; Nakajima, K.; Suzuki, M.; Tsuji, H.; Kimura, K. *Surf. Sci.* **2010**, *604*, 464−469.
(40) Fortunato, R.; Afonso, C. A. M.; Benavente, J.; Rodriguez-Castellon, E.; Crespo, J. G. *J. Membr. Sci.* **2005**, *256*, 216−223.
(41) Smith, E. F.; Garcia, I. J. V.; Briggs, D.; Licence, P. *Chem. Commun.* **2005**, 5633−5635.
(42) Smith, E. F.; Rutten, F. J. M.; Villar-Garcia, I. J.; Briggs, D.; Licence, P. *Langmuir* **2006**, *22*, 9386−9392.
(43) Gottfried, J. M.; Maier, F.; Rossa, J.; Gerhard, D.; Schulz, P. S.; Wasserscheid, P.; Steinrück, H.-P. *Z. Phys. Chem.* **2006**, *220*, 1439−1453.
(44) Silvester, D. S.; Broder, T. L.; Aldous, L.; Hardacre, C.; Crossley, A.; Compton, R. G. *Analyst* **2007**, *132*, 196−198.
(45) Caporali, S.; Bardi, U.; Lavacchi, A. *J. Electron Spectrosc. Relat. Phenom.* **2006**, *151*, 4−8.
(46) Santos, C. S.; Baldelli, S. *J. Phys. Chem. B* **2007**, *111*, 4715−4723.
(47) Krischok, S.; Eremtchenko, M.; Himmerlich, M.; Lorenz, P.; Uhlig, J.; Neumann, A.; Öttking, R.; Beenken, W. J. D.; Höfft, O.; Bahr, S.; Kempter, V.; Schaefer, J. A. *J. Phys. Chem. B* **2007**, *111*, 4801−4806.
(48) Lockett, V.; Sedev, R.; Bassell, C.; Ralston, J. *Phys. Chem. Chem. Phys.* **2008**, *10*, 1330−1335.
(49) Maier, F.; Gottfried, J. M.; Rossa, J.; Gerhard, D.; Schulz, P. S.; Schwieger, W.; Wasserscheid, P.; Steinrück, H.-P. *Angew. Chem., Int. Ed.* **2006**, *45*, 7778−7780.
(50) Shirley, D. A. *Phys. Rev.* **1972**, *B5*, 4709−14.
(51) Matsumoto, K.; Tsuda, T.; Nohira, T.; Hagiwara, R.; Ito, Y.; Tamada, O. *Acta Crystallogr.* **2002**, *C58*, m186−m187.
(52) te Velde, G.; Bickelhaupt, F. M.; Baerends, E. J.; Guerra, C. F.; Van Gisbergen, S. J. A.; Snijders, J. G.; Ziegler, T. *J. Comput. Chem.* **2001**, *22*, 931−967.
(53) Guerra, C. F.; Snijders, J. G.; Te Velde, G.; Baerends, E. J. *Theor. Chem. Acc.* **1998**, *99*, 391−403.
(54) ADF 2004.01, SCM, Theoretical Chemistry, Vrije Universiteit: Amsterdam, The Netherlands (http://www.scm.com).
(55) Adachi, H.; Tsukada, M.; Satoko, C. *J. Phys. Soc. Jpn.* **1978**, *45*, 875.
(56) Kurisaki, T.; Nakazono, Y.; Matsuo, S.; Perera, R. C. C.; Underwood, J. H.; Wakita, H. *Adv. Quantum Chem.* **2008**, *54*, 315−323.
(57) Kurisaki, T.; Matsuo, S.; Tóth, I.; Wakita, H. *Anal. Sci.* **2008**, *24*, 1385−1392.
(58) Dedryvère, R.; Leroy, S.; Martinez, H.; Blanchard, F.; Lemordant, D.; Gonbeau, D. *J. Phys. Chem. B* **2006**, *110*, 12986−12992.
(59) Scofield, J. H. *J. Electron Spectrosc. Relat. Phenom.* **1976**, *8*, 129−37.
(60) Iwahashi, T.; Nishi, T.; Yamane, H.; Miyamae, T.; Kanai, K.; Seki, K.; Kim, D.; Ouchi, Y. *J. Phys. Chem. C* **2009**, *113*, 19237−19243.